

## **A SIMPLE FRACTURE MECHANICS MODEL FOR MIXED-MODE FAILURE IN CONCRETE**

T. Olofsson and U. Ohlsson,

Division of Structural Engineering, Luleå University of Technology,  
Luleå, Sweden

M. Klisinski,

Division of Engineering Mechanics, Luleå University of Technology,  
Luleå, Sweden

### **Abstract**

A simple fracture mechanics model is presented based on the fictitious crack concept where the crack initiation is controlled by a failure surface in the normal and shear stress space. The postfailure behaviour is controlled by a softening isotropic kinematic rule based on the effective stress-crack opening deformation. The model in its simplest configuration needs only four parameters, the uniaxial tensile and compressive strengths, the value of fracture energy ( $G_f$ ) and a constant controlling the isotropic softening of the yield surface. The model has been implemented in the inner softening band approach where a strong discontinuity is included in the element formulation.

### **1 Introduction**

The inner softening band (ISB) has been presented by Klisinski et al. (1991), Olofsson et al. (1994) and Klisinski et al. (1995). The major advan-

tage of the ISB approach is that discrete cracks can be introduced anywhere and in any direction within the finite element mesh. Since, the ISB approach is based on traction versus displacements the fictitious crack approach can directly be implemented. Models based on this concept lump the physical behaviour in the fracture process zone to a fracture surface. The required parameters can often directly be determined from material tests.

## 2 A general model for mixed mode fracture

The mixed mode cracking of concrete can be divided into an initiation part, (orientation and location) and a crack evolution part based on the constitutive relation between tractions and crack opening displacements.

### 2.1 Crack initiation

The crack initiation criteria is described by a parabola in the normal and shear stress space, see Fig. 1:

$$F = \alpha_o \tau^2 + \sigma - \sigma_o \quad (1)$$

The two constants  $\sigma_o$  and  $\alpha_o$  can be evaluated from two tests. Given the uniaxial tensile strength,  $f_t$ , and the uniaxial compression strength,  $f_c$ ,  $\sigma_o$  and  $\alpha_o$  can be evaluated as:

$$\alpha_o = \frac{1}{f_t \left( 2 + f_c/f_t - 2\sqrt{1 + f_c/f_t} \right)} ; \sigma_o = f_t \quad (2)$$

Denoting  $p = (\sigma_1 + \sigma_2)/2$  and  $q = (\sigma_1 - \sigma_2)/2$  the crack initiation condition can be described in the biaxial stress space as:

$$F = \alpha_o q^2 + p + \frac{1}{4\alpha_o} - \sigma_o \quad (3)$$

The crack direction  $\theta$  can be calculated from the condition that the tangent of the crack initiation surface and the tangent of Mohr's circle shall be equal at the point of contact, i.e.:

$$\sin \phi = \frac{1}{2\alpha_o q} \quad (4)$$

The crack direction  $\sin\phi \in [0,1]$  limits the value of  $q \in [\infty, 1/(2\alpha_o)]$ . From the condition  $F = 0$  in Eq. (3) the limiting values of the mean stress  $p \in [-\infty, f_t - 1/(2\alpha_o)]$  is found. For values of  $p > f_t - 1/(2\alpha_o)$  Eq. (3) is replaced by the Rankine criteria:

$$F = \sigma_1 - f_t \quad (5)$$

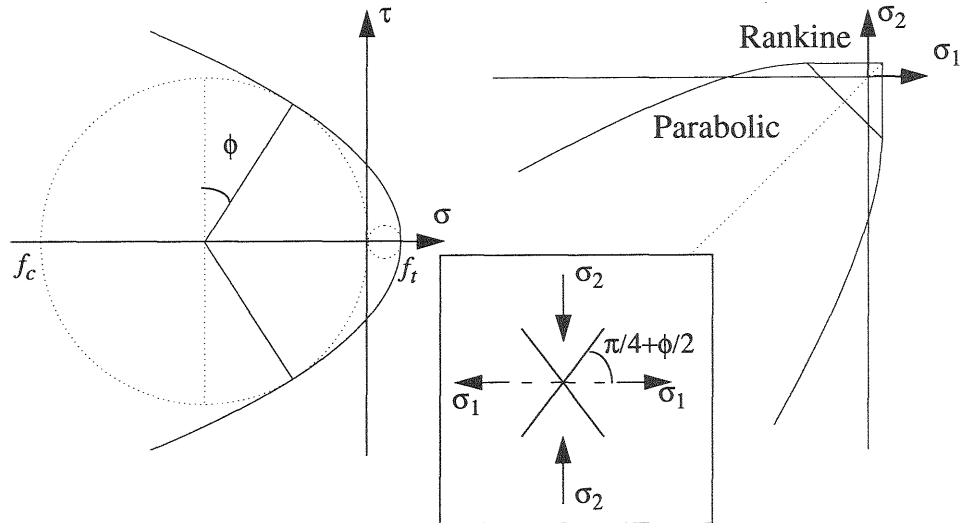


Fig. 1. Parabolic crack initiation criteria.

## 2.2 Crack evolution law

After the crack has been formed it is essential to establish the evolution of the crack displacements as a function of the traction acting on the crack surface. In the spirit of the fictitious crack model, Hillerborg et al. (1976), the initial yield surface describing the condition between tractions on the crack plane is modified as the crack opens or shears and shrink to its residual form. Therefore, softening is described in terms of tractions  $\mathbf{t}$  versus relative crack displacement  $\mathbf{u}$ , see Fig. 2, where indices  $n$  and  $s$  denote the normal and shear component with respect to the crack plane. The shape of the yield surface coincides with the assumed crack initiation surface.

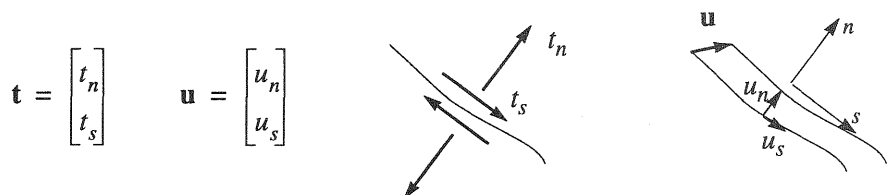


Fig. 2. Definition of traction and relative crack displacement

However, the parameters  $\sigma_o \rightarrow \sigma_e(u_e)$  and  $\alpha_o \rightarrow \alpha_e(u_e)$  will now be a function of the effective relative displacement:

$$F = \alpha_e(u_e) \tau^2 + \sigma - \sigma_e(u_e) \tag{6}$$

$$u_e = \|\mathbf{u}\| = \sqrt{\mathbf{u}^T \mathbf{u}} = \sqrt{u_n^2 + u_s^2}$$

The parameters  $\sigma_e(u_e)$  and  $\alpha_e(u_e)$  describe the kinematic and isotropic softening of the yield surface, respectively, see Fig. 3.

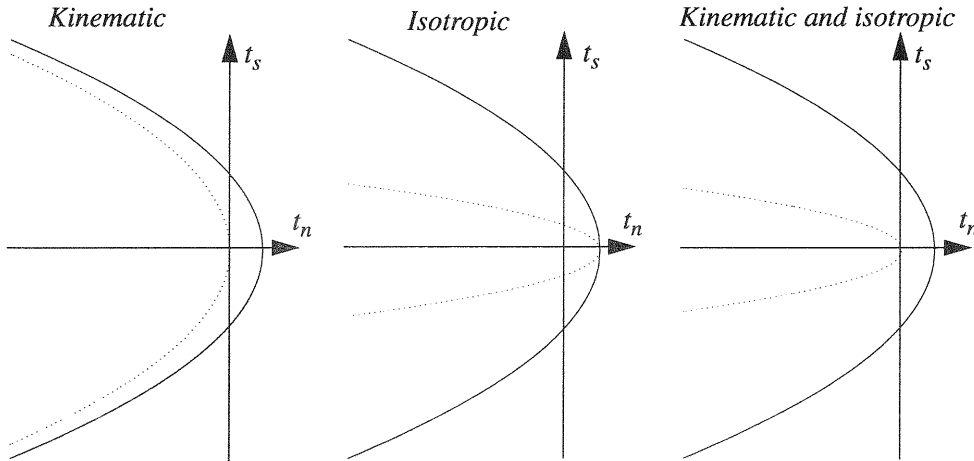


Fig. 3. Kinematic and isotropic softening of the yield surface.

The relations  $\sigma_e(u_e)$  and  $\alpha_e(u_e)$  describe the softening law. They can be chosen as linear or nonlinear, see Fig. 4.

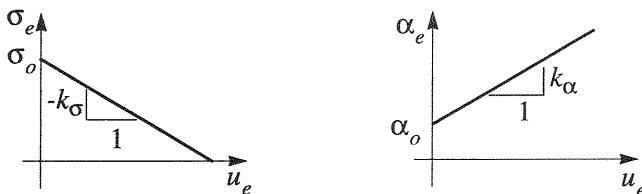


Fig. 4. Example on linear softening laws.

### 2.3 Flow rule and the consistency equation

Adopting the incremental theory of plasticity we now specify a flow rule and use the consistency condition to evaluate the relation between tractions and relative crack displacements on rate form. The relative crack opening displacements are assumed to follow an associated flow rule:

$$\dot{\mathbf{u}} = \dot{\lambda} \mathbf{n} = \dot{\lambda} \frac{\partial F}{\partial \mathbf{t}} ; \mathbf{n} = \begin{bmatrix} 1 \\ 2\alpha_e t_s \end{bmatrix} \quad (7)$$

The consistency condition can be written:

$$\dot{F} = \mathbf{n}^T \dot{\mathbf{t}} - h \dot{\lambda} = 0 \Rightarrow \dot{\lambda} = \frac{\mathbf{n}^T \dot{\mathbf{t}}}{h} \quad (8)$$

where  $h = -(k_\sigma + k_\alpha t_s^2) \sqrt{\mathbf{n}^T \mathbf{n}}$ . Using Eq. (8) in the flow rule gives the relation between tractions and crack opening displacements on rate form as:

$$\dot{\mathbf{u}} = \frac{\mathbf{n} \mathbf{n}^T}{h} \dot{\mathbf{t}} = \mathbf{C} \dot{\mathbf{t}} ; \mathbf{C} = \frac{1}{-(k_\sigma + k_\alpha t_s^2) \sqrt{1 + 4\alpha_e t_s^2}} \begin{bmatrix} 1 & 2\alpha_e t_s \\ 2\alpha_e t_s & 4\alpha_e t_s^2 \end{bmatrix} \quad (9)$$

### 3 Finite element with inner softening band

The concept of the ISB element is based on the decomposition of the nodal displacements rates  $\dot{\mathbf{v}}$  into two parts, one related to the continuum and one corresponding to the softening band

$$\dot{\mathbf{v}} = \dot{\mathbf{v}}^c + \dot{\mathbf{v}}^d \quad (10)$$

Here  $\dot{\mathbf{v}}^c$  is the nodal displacement rate caused by the deformation of the continuous part of the element and  $\dot{\mathbf{v}}^d$  is attributed to the discontinuity within the element at the location of the softening band. The contribution from the inner softening band is coupled to the nodal deformation rates via the redistribution matrix  $\mathbf{A}$ , see Fig. 5:

$$\dot{\mathbf{v}} = \mathbf{A} \mathbf{q} \dot{\mathbf{u}} \quad \mathbf{q} = \begin{bmatrix} -s & c \\ c & s \end{bmatrix} \quad \begin{array}{l} s = \sin \theta \\ c = \cos \theta \end{array} \quad (11)$$

Here  $\mathbf{q}$  is the transformation matrix rotating the local ISB displacements

$$\mathbf{A}^T = \begin{bmatrix} -\beta & 0 & -\beta & 0 & 1-\beta & 0 \\ 0 & -\beta & 0 & -\beta & 0 & 1-\beta \end{bmatrix} \quad \begin{array}{c} \text{Diagram 1: Triangle with nodes } i, j, k \text{ and a horizontal band } k \text{ at the top.} \\ \text{Diagram 2: Triangle with nodes } i, j, k \text{ and a horizontal band } k \text{ at the bottom.} \end{array}$$

$$\mathbf{A}^T = \begin{bmatrix} -1+\beta & 0 & \beta & 0 & \beta & 0 \\ 0 & -1+\beta & 0 & \beta & 0 & \beta \end{bmatrix}$$

Fig. 5. Redistribution matrix

to the element coordinate system. The redistribution matrix  $\mathbf{A}$  for a CST element can have one of the following forms depending on the location of the discontinuity. The parameter  $\beta \in [0, 1]$  defines the relative distance of the discontinuity within the element, hence the  $\mathbf{A}$  matrix represents a unit jump at the location of the discontinuity. It is possible to define for such an element the equivalent “plastic strain” as follows:

$$\dot{\epsilon}^p = \mathbf{B}\mathbf{A}\mathbf{q}\dot{\mathbf{u}} = \mathbf{B}\mathbf{A}\mathbf{q}\dot{\lambda}\mathbf{n} = \dot{\lambda}\bar{\mathbf{m}} \quad \bar{\mathbf{m}} = \mathbf{B}\mathbf{A}\mathbf{q}\mathbf{n} \quad (12)$$

where  $\mathbf{B}$  is the standard matrix containing spatial derivatives of the shape functions. The traction rate vector  $\dot{\mathbf{t}}$  at the discontinuity can be calculated from the element stress rates as

$$\dot{\mathbf{t}} = \mathbf{Q}\dot{\boldsymbol{\sigma}} \quad \mathbf{Q} = \begin{bmatrix} s^2 & c^2 & -2sc \\ -sc & sc & c^2 - s^2 \end{bmatrix} \quad \begin{array}{l} s = \sin\theta \\ c = \cos\theta \end{array} \quad (13)$$

where  $\mathbf{Q}$  represents the transformation matrix to the discontinuity coordinate system. The angle  $\theta$  describes how much the discontinuity is rotated with respect to the horizontal plane. For the CST element further calculations can be made in a way similar to the standard plasticity approach. Writing down the strain increment and the consistency condition

$$\dot{\boldsymbol{\epsilon}} = \dot{\boldsymbol{\epsilon}}^e + \dot{\boldsymbol{\epsilon}}^p = \mathbf{D}^{-1}\dot{\boldsymbol{\sigma}} + \bar{\mathbf{m}}\dot{\lambda} \quad (14)$$

$$0 = \dot{F} = \mathbf{n}^T\dot{\mathbf{t}} - h\dot{\lambda} = \mathbf{n}^T\mathbf{Q}\dot{\boldsymbol{\sigma}} - h\dot{\lambda} = \bar{\mathbf{n}}^T\dot{\boldsymbol{\sigma}} - h\dot{\lambda}$$

the following system is obtained

$$\begin{bmatrix} \dot{\boldsymbol{\epsilon}} \\ 0 \end{bmatrix} = \begin{bmatrix} \mathbf{D}^{-1} & \bar{\mathbf{m}} \\ \bar{\mathbf{n}}^T & h \end{bmatrix} \begin{bmatrix} \dot{\boldsymbol{\sigma}} \\ \dot{\lambda} \end{bmatrix} \quad (15)$$

where  $\mathbf{D}$  is the elastic stiffness matrix,  $h$  is the “plastic” modulus and

$$\bar{\mathbf{m}} = \mathbf{B}\mathbf{A}\mathbf{q}\mathbf{n} ; \bar{\mathbf{n}} = \mathbf{Q}^T\mathbf{n} \quad (16)$$

Solving Eq. (15), considering that the plastic modulus,  $h$ , is zero for ideal plasticity, gives:

$$\dot{\boldsymbol{\sigma}} = \left( \mathbf{D} - \frac{\mathbf{D}\bar{\mathbf{m}}\bar{\mathbf{n}}^T\mathbf{D}}{h + \bar{\mathbf{n}}^T\mathbf{D}\bar{\mathbf{m}}} \right) \dot{\boldsymbol{\epsilon}} = \mathbf{D}^{ep}\dot{\boldsymbol{\epsilon}} \quad (17)$$

Note that  $\bar{\mathbf{n}} = \bar{\mathbf{m}}$  only if  $\mathbf{B}\mathbf{A}\mathbf{q} = \mathbf{Q}^T$ . This happens only if the discontinuity

is parallel to one of the element sides. As a result the stiffness matrix  $\mathbf{D}^{ep}$  is non-symmetric in general.

#### 4 Comparison with mixed-mode tests on concrete

Recall, that the required parameters for the crack initiation parabola can be determined from the uniaxial tensile and compressive strength,  $f_t$  and  $f_c$ . The kinematic softening evaluation law must in the case of mode I coincide with the softening behaviour in a uniaxial tension test. One such simple relationship which requires only one additional material parameter, the fracture energy ( $G_f$ ), is the following exponential equation:

$$\sigma_e = f_t e^{\left(\frac{f_t}{G_f}\right)u_e} \quad (18)$$

For the isotropic softening, i.e. the change of  $\alpha$ , a linear relationship of the effective crack deformation  $u_e$  has been selected. The parameter left to determine which is not directly accessible from experiments will be the slope of the curve  $k_\alpha$ , see Fig. 4. Let's take an ordinary concrete with the material parameters shown in Fig. 6 and do a single element test in order to evaluate the features of the proposed model. First the element is loaded in pure mode I until a crack is initiated in the element. Then the element is loaded with an angle to introduce a shear component. Fig 7. shows the tractions versus the crack opening displacement over the discontinues softening band in the element as a function of the angle  $\beta$ , the size of the element and the parameter  $k_\alpha$ . At first it might seem strange that the element size will influence the crack behaviour. However, since the control is based on nodal displacement a discontinuity in a larger element will be less confined compared to a smaller one.

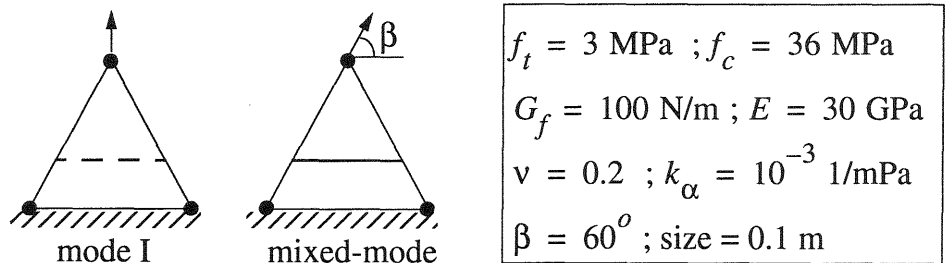


Fig. 6. A single element test, default values to the right

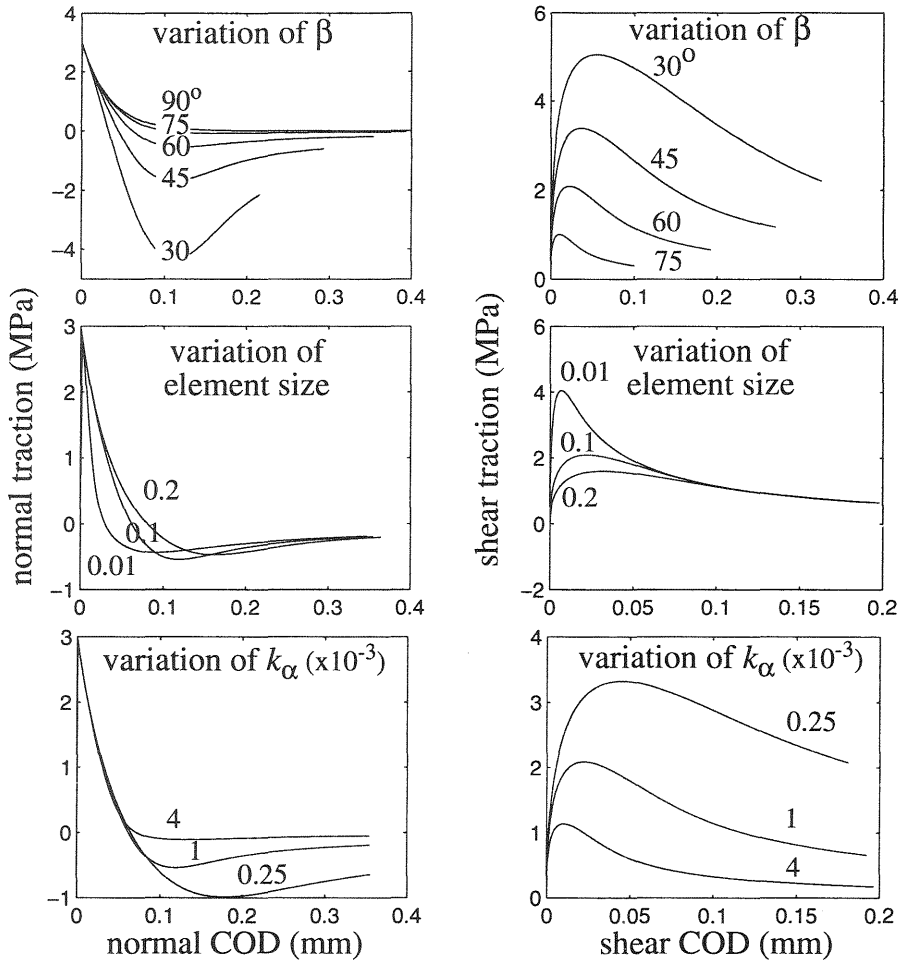


Fig. 7. Normal and shear tractions versus crack opening displacements, (COD) for varying angle  $\beta$ , the size of the element and the parameter  $k_\alpha$ .

To check the validity of the model and to get some indication of the parameter  $k_\alpha$  the test from mixed mode tests on concrete made by Hassanzadeh (1992) will be compared to the behaviour of a single ISB element. Hassanzadeh performed displacement controlled tests on notched concrete cubes in two steps. In the first step the specimen was loaded in pure mode I until the maximum load was attained. In the second step the control was switched to a linear or a parabolic relation between the normal and shear displacement. Fig. 8 shows the setup and the selected material data. The only parameter selected to fit the experiments is the value of  $k_\alpha$ .

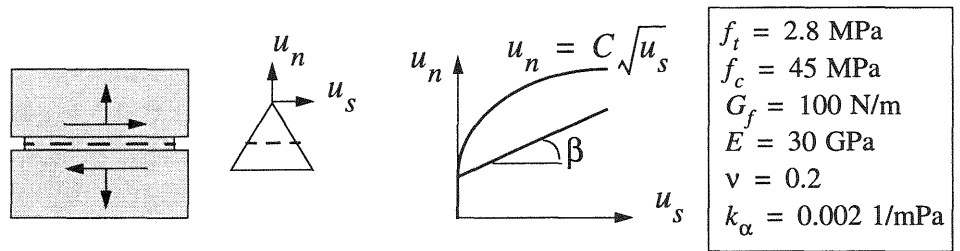


Fig. 8. Comparison with mixed-mode experiments on concrete. The size of the element was set to half the specimen height (30 mm).

The outcome of the comparison is shown in Fig 9. Although the result is not in total agreement especially for the parabolic path, the basic behaviour is represented quite well. Better agreement can certainly be obtained for example by changing the shape of the yield surface, introducing more sophisticated softening rules etc., however at the expense of increasing the complexity of the model.

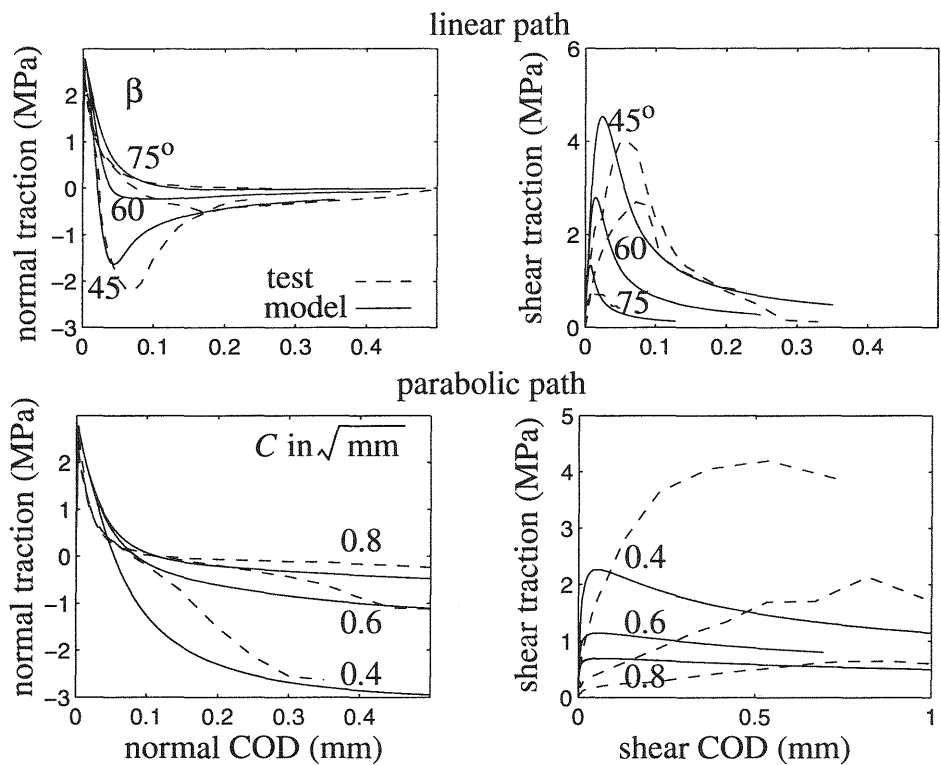


Fig. 9. Model output compared with mixed-mode test on concrete performed by Hassanzadeh (1992).

## 5 Conclusion

A simple physical mixed-mode model in the spirit of the fictitious crack approach has been suggested and implemented in the inner softening band method. Since the constitutive assumption is based on tractions versus displacements, the model can also be applied to interface elements. Comparing single element tests with experimental data suggests that the basic features of mixed-mode cracking are captured. The model has also been applied in finite element calculations of concrete structures, see Ohlsson et al. (1995) and Noghabai (1995).

## 6 Acknowledgement

The work was supported by the Swedish Research Council for Engineering Sciences, grant 261/94-61. The experimental data on mixed-mode test on concrete was provided by Dr. Manouchehr Hassanzadeh. The work was supervised by Prof. Lennart Elfgren

## 7 References

- Hassanzadeh, M. (1992) **Behaviour of fracture process zones in concrete influenced by simultaneously applied normal and shear displacements**. Doctoral thesis TVBM-1010, Lund Institute of Technology, Sweden.
- Hillerborg, A., Modeer, M. and Petersson P-E (1976) Analysis of crack formation and crack growth in concrete by means of fracture mechanics and finite elements. **Cement and Concrete Research**, 6, 773-782.
- Klisinski, M., Olofsson, T. and Tano, R. (1995) Mixed mode cracking of concrete modelled by inner softening band., **Computational Plasticity** (eds D.R.J. Owen et al.), Pineridge Press, Swansea, U.K., 1595-1606.
- Klisinski, M., Runesson K. and Sture, S. (1991) Finite element with inner softening band. **Journal of Engineering Mechanics**, 3, 575-587.
- Noghabai K. (1995) Splitting of concrete covers - a fracture mechanics approach, in this volume
- Ohlsson, U., Olofsson, T. (1995) Anchor bolts in concrete structures, finite element calculations based on inner softening bands, in this volume.
- Olofsson, T., Klisinski, M. and Nedar P. (1994) Inner softening band: A new approach to localization in finite elements, in **Computational Modelling of Concrete Structures** (eds H. Mang et al.), Pineridge Press Ltd., Swansea, U.K., 373-382.